Int. J. Heat Mass Transfer. Vol. 28, No. 8, pp. 1539–1549, 1985
Printed in Great Britain

0017-9310/85 $3.00 + 0.00

Electrostatic characteristics of a charged turbulent free jet

B. ABEDIAN, ERIC S. DAVIS
Mechanical Engineering Department, Tufts University, Medford, MA, U.S.A.

and

M. METGHALCHI
Mechanical Engineering Department, Northeastern University, Boston, MA 02115, U.S.A.

(*Received* 10 *February* 1984 *and in final form* 20 *February* 1985)

Abstract—The spreading and decaying of a charged fluid that is issued into a stagnant fluid as an unconstraint-submerged turbulent jet is investigated. The dynamic conservation equation of charge is solved analytically for the mean charge density field in the flow by assuming a simple velocity field and numerically by using a more accurate velocity field. It is shown that the characteristics of a charged jet can be described by a dimensionless length ratio defined as $\varepsilon V_j/\sigma a_j$ with ε and σ being the fluid electrical permittivity and the fluid electrical conductivity, respectively. Based on the electrostatic properties of a charged jet, three conductivity ranges were identified. In the high-conductivity range, when $\sigma > 0.2\,\varepsilon V_j/a_j$, the charged region is confined only to the near field. In the other extreme, for $\sigma < 0.002\,\varepsilon V_j/a_j$, there is a low-conductivity range in which the charge density field in the flow behaves analogously to other conservative scalar field properties in a turbulent jet with similar rates of decay and spread. The intermediate conductivity range falls between these two limits and here charge dispersion is controlled by migration and diffusion.

INTRODUCTION

CHARGING in fluids is an observable phenomenon on a macroscopic level whenever the fluid conductivity is very low. A charged species is transported in fluid media by convection, diffusion and migration. Ordinary solute solutions and water have relatively high conductivities, and with respect to a length scale of the flow geometry, migration predominates the transport phenomenon. In other words, the time scale for migration of charge is much smaller than the corresponding time scales for convection and diffusion; and as a result, diffusion or convection of charge in the flow is virtually nonexistent. For such fluids, it is only in the close vicinity of an interface that all the time scales may become of the same order and the three effects have to be considered simultaneously [1]. In a nearly insulating liquid, on the other hand, the migration time scale is usually of the order of a few seconds and longer. Charge can thus be transported in an insulating liquid via convection and/or diffusion in a macro-length scale. Convective charge transfer is of interest to scientists and engineers because of electrostatic hazards associated with charging in hydrocarbon fuels [2, 3].

In fuel transport operations, the fluid which is charged by passing through pipes and filters enters the receiving tank frequently as a turbulent jet. The purpose of this paper is to find the properties of a charge density fluid which is generated in charged, turbulent, free jet flow. The rates of spread and decay of the charge density field contribute to a more accurate prediction of electrostatically hazardous situations that may occur in the receiving tank [4].

For a turbulent jet issued into a stagnant fluid, experimental and theoretical studies are available on the properties of a mean scalar field $\Gamma(r, z)$ such as temperature and mass concentration [5–12]. These analyses are based on the argument that the mean property profiles are self-preserved at least after a specific length from the origin of the jet. It is then concluded that the profiles obey a decay law for the mean property at the centerline denoted by Γ_c which is of the form

$$\frac{\Gamma_j}{\Gamma_c} = C_1(z-z')/a_j \tag{1}$$

and the half-radius $r_{1/2}$ which is a distance from the centerline where $\Gamma(r_{1/2}, z) = \frac{1}{2}\Gamma_c$ grows according to

$$r_{1/2} = C_2(z-z'). \tag{2}$$

In these equations, Γ_j is the mean property at the origin, a_j is the nozzle radius, and C_1 and C_2 and z' are constants of the order 0.1, 0.1 and 10 a_j, respectively.

Because of migration of charge, the dynamic conservation equation for charge density contains an additional term which is absent in the conservation equation for conservative properties such as mass and energy. An extra length scale is then required to fully define a charge density field; and it may thus be concluded that the charge density field can not be characterized by a self-preservation hypothesis. As a result of this distinction, it is expected that in general equations (1) and (2) do not describe the spread and decay of a charge density field in turbulent free jets.

Schon and Kramer [13] have considered the flow

NOMENCLATURE

a_j jet radius at the inlet section
C concentration of species
C_1 a constant in decay law
C_2 a constant in spread law
D molecular diffusion coefficient
D_{ij} turbulent diffusion tensor
D_T turbulent eddy-diffusion in radial direction
F Faraday's constant
J current density
K a constant in the expression for D_T
L_c dimensionless parameter, $\tau v_j/a_j$
Pe Péclet number
q local charge density
q' charge density fluctuating component
r radial coordinate
$r_{1/2}$ half-radius
r_1 inner radius of the diffuse layer
r_2 outer radius of the diffuse layer
Re Reynolds number
Sc Schmidt number
t time
V velocity field
v velocity component
v' fluctuating velocity component
x_j coordinate in j-direction
Z charge number
z axial coordinate
z_i length of the inlet section
z_f length of the inlet and transitional sections
z' a constant in the decay and spread similarity laws.

Greek symbols
α rate of growth of the diffuse layer
Γ scalar field property
ε fluid's electric permittivity
κ mobility of ionic species
λ the Debye length
ν viscosity
ν_T turbulent eddy-viscosity
σ fluid's conductivity
τ relaxation time
χ normalized radial component in the diffuse layer
ψ electric potential.

Subscripts
c centerline of jet
i index
j jet inlet
0 electrically undisturbed fluid
+ positive charge
− negative charge.

field generated by a point source in one, two and three dimensions and obtained charge density distributions in the moving fluid. In their theoretical study, however, the effect of diffusion is ignored; and as a result, Schon and Kramer's analysis does not distinguish between the cases of laminar and turbulent flows, nor can it predict when diffusion may play a dominant role in charge dispersion. Specifically, in turbulent flows, where turbulent diffusion is present, their theory has a very limited application.

THE GOVERNING EQUATIONS

The local current density vectors $\mathbf{J}_+$ and $\mathbf{J}_-$, which are present in a fluid due to displacement of positive and negative ionic species, respectively, are written as

$$\mathbf{J}_\pm = FZ_\pm[C_\pm\mathbf{V} - D_\pm\nabla C_\pm - Z_\pm C_\pm\kappa_\pm\nabla\psi] \quad (3)$$

where F is the Faraday constant, Z is the charge number, C is the species concentration, $\mathbf{V}$ is the local velocity vector, D and κ are the molecular diffusion coefficient and the mobility of ionic species respectively, and ψ is the local electric potential. Subscripts + and − refer to positive and negative ions. The three terms on the RHS of equation (3) represent the contributions of convection, diffusion and migration phenomena to the current densities.

Simplifying assumptions will be made to obtain the equation for the net current density from equation (3). It will be assumed that all the ionic species are univalent, i.e. $Z_+ = -Z_- = 1$, and that the diffusion coefficient of positive and negative ions are equal, i.e. $D_+ = D_- = D$. In case of inequality of diffusion coefficients, D may be considered to be the average molecular diffusion coefficient. By further assuming that $\kappa_+ = \kappa_- = \kappa$, we are essentially considering a binary solution of identical physico-chemical properties for the charged species. Using equation (3), the net current density which is defined as

$$\mathbf{J} = \mathbf{J}_+ + \mathbf{J}_- \quad (4)$$

will take the form

$$\mathbf{J} = \mathbf{V}\cdot q - D\nabla q - \sigma\nabla\psi \quad (5)$$

where q is the local charge density which is generated due to an imbalance of the concentrations of positive and negative ionic species,

$$q = F(C_+ - C_-), \quad (6)$$

and σ is the fluid conductivity which is related to C_+

and C_-;

$$\sigma = F\kappa(C_+ + C_-). \tag{7}$$

A comparison of equations (6) and (7) reveals that in general σ is dependent on the charge density field q and is therefore itself a field property. The small charge density limit is referred to a state of the fluid when

$$|q/FC_0| \ll 1, \tag{8}$$

with C_0 being the concentration of charged species in an electrically undisturbed fluid. In such a limit, the concentration of charged species is not affected dramatically even when the fluid is charged and we can write

$$C_+ + C_- \simeq C_0,$$

with C_0 being the concentration of ionic species in an undisturbed fluid, everywhere in the flow. Consequently, in the small charge density limit which is described by equation (8), we have

$$\sigma \simeq \sigma_0 \equiv F\kappa C_0 \tag{9}$$

which means that the fluid conductivity is invariant throughout the flow region and is equal to the conductivity of the fluid σ_0 in an electrically neutral state. To eliminate $\mathbf{J}$ and ψ from equation (5), the equation of continuity of charge

$$\frac{\partial q}{\partial t} + \nabla \cdot \mathbf{J} = 0, \tag{10}$$

with t being the time and the Poisson's equation,

$$\nabla^2 \psi = -\frac{q}{\varepsilon}, \tag{11}$$

with ε being the fluid permittivity, will be used. Once equations (5), (10) and (11) are combined together, the continuity equation for an incompressible fluid,

$$\nabla \cdot \mathbf{V} = 0, \tag{12}$$

can be applied to obtain the transport equation which is the dynamic conservation equation of charge.

$$\frac{\partial q}{\partial t} + \mathbf{V} \cdot \nabla q - \nabla \cdot D\nabla q + \frac{1}{\tau} q = 0. \tag{13}$$

Here

$$\tau \equiv \frac{\varepsilon}{\sigma} \tag{14}$$

is the relaxation time for charge migration in fluids. The term q/τ takes into account the migration of charge as a result of the induced electric field in the fluid and in the absence of convection and diffusion leads to a simple exponential decay of charge with a characteristic time constant τ.

In a typical dynamic equation for conservation of a quantity such as mass or energy, the last term in equation (13) is absent. It then appears that equation (13) describes the conservation equation of a non-conservative quantity which is depleting at a rate of q/τ. In fact, in flows with chemical reaction, if one of the species experiences a first-order reaction with negligible temperature dependency, the corresponding production term is linear and the conservation equation of that species will be analogous to equation (13) [14]. It may thus be concluded that the present analysis which is for a turbulent charged jet could be applied to predict the characteristics of a turbulent reacting jet provided that the conditions mentioned above exist.

Electrostatic body forces are present in the fluid because of the induced electric field. However, these forces are always much smaller than the rate of change of fluid momentum in the small charge density limit which then indicates that the electrostatic body forces do not disturb the flow field. Accordingly, it will be assumed that the flow field is independent of the charge density field and is similar to the case of an uncharged fluid. Taking this assumption into consideration, equation (13) then becomes linear in q. A case in which electrostatic body forces initiate a turbulent jet of charged fluid is discussed by Bailey and Balachandran [15].

In turbulent flows, a field properly is considered to be the sum of two components, an averaged-mean component and a fluctuating component. Perturbing the charge density field as $q = \bar{q} + q'$, with $\bar{q}$ being the mean charge density and q' being the fluctuating part, the transport equation can then be written for $\bar{q}$ as follows

$$\frac{\partial \bar{q}}{\partial t} + \bar{V} \cdot \nabla \bar{q} - \nabla \cdot \left(D_{ij} \frac{\partial \bar{q}}{\partial x_j} \right) - \nabla \cdot D\nabla \bar{q} + \frac{\bar{q}}{\tau} = 0 \tag{15}$$

where $\bar{V}$ is the mean velocity field and

$$D_{ij} \equiv \frac{\overline{v_i' q'}}{\partial \bar{q}/\partial x_j} \tag{16}$$

is a turbulent diffusion tensor, with v_i' being the ith component of the turbulence velocity. Making a boundary-layer-type approximation, we neglect the axial diffusion of charged species and further we drop out the axial convection due to turbulence. For a steady axi-symmetric circular jet, the final equation is then given by

$$\mathbf{V} \cdot \nabla q - \frac{1}{r} \frac{\partial}{\partial r} \left[r(D + D_T) \frac{\partial q}{\partial r} \right] + \frac{q}{\tau} = 0 \tag{17}$$

with D_T being the turbulent-eddy diffusion coefficient of charged species in the radial direction and r being the radial component. In this equation, overbars referring to the averaged properties are omitted.

It is evident that because of one additional time scale the governing equation, that is τ, the charge density profiles in jet flows do not obey a self-preservation law. Nonetheless, there are dimensionless parameters which characterize the charge density field in the flow. One such parameter is the Reynolds's number, $Re \equiv 2V_j a_j/\nu$ with V_j being the initial jet velocity, a_j being the initial jet radius and ν being the kinematic viscosity, which

specifies the velocity field V(r, z) and the eddy-diffusion coefficient D_T. From equation (17), two other parameters can be deduced: a dimensionless length scale which describes the molecular diffusion of charged species and in surface chemistry is known as the Debye ratio,

$$\lambda \equiv \sqrt{\tau D}/a_j \tag{18}$$

and another length scale which characterizes the convection of charged species and is defined as

$$L_c \equiv \frac{\tau V_j}{a_j}. \tag{19}$$

Now, assuming that the charge density of the fluid is initially q_j, the nondimensionalized version of equation (17) can be obtained as follows

$$L_c v_z^* \frac{\partial q^*}{\partial z^*} + L_c v_r^* \left(\frac{\partial q^*}{\partial r^*} + \frac{q^*}{r^*}\right) - \frac{\lambda^2}{r^*}\frac{\partial}{\partial r^*}\left[r^*\left(1+\frac{D_T}{D}\right)\frac{\partial q^*}{\partial r^*}\right] + q^* = 0. \tag{20}$$

Here, $V^* = v/V_j$ is the dimensionless velocity, $r^* = r/a_j$ and $z^* = z/a_j$ are the dimensionless spatial components, and $q^* = q/a_j$ is the dimensionless charge density. We ignore the double-layer effect on the walls of the receiving tank which may interfer with the charged jet; also we assume that the fluid has a uniform charge density at the inlet. Accordingly, the initial and boundary conditions for $q^*(r^*, z^*)$ will be

$$\begin{aligned} q^*(r^*, 0) &= 1 \quad r^* \leqslant 1 \\ q^*(r^*, 0) &= 0 \quad r^* > 1. \end{aligned} \tag{21}$$

Symmetry condition exists on the jet axis and q^* vanishes at large r^* and z^*.

We further use the approximation that the turbulent Schmidt number is unity. In the particular case of a turbulent jet where the turbulent eddy diffusion coefficient is a constant over the entire flow domain, we may write

$$D_T = \nu_t = \kappa V_j a_j \tag{22}$$

where κ is a constant which is determined experimentally. For computational purposes, we set $\kappa = 0.024$ [16]. Using equation (22), the ratio D_T/D can be expressed in terms of the Peclet number Pe of the flow;

$$\frac{D_T}{D} = \kappa Pe = \kappa L_c/\lambda^2 \tag{23}$$

with $Pe \equiv V_j a_j/D$ being the product of Re and $Sc = \nu/D$ which is the Schmidt number. Generally, for hydrocarbon liquids, Sc for charged species is of the order of 10^3. Consequently, Pe becomes much larger than unity which in turn indicates that in our case of concern molecular diffusion can be neglected in comparison to turbulent diffusion. Substitution of D_T/D in equation (20) results

$$V_z^* \frac{\partial q^*}{\partial z^*} + V_r^*\left(\frac{\partial q^*}{\partial r^*} + \frac{q^*}{r^*}\right) - \frac{\kappa}{r^*}\frac{\partial}{\partial r^*}\left(r^*\frac{\partial q^*}{\partial r^*}\right) + \frac{1}{L_c}q^* = 0. \tag{24}$$

In turbulent jets, V_z^* and V_r^* are independent of Re. It thus becomes evident that, in circular, turbulent charged jets, q^* can be characterized by only one dimensionless parameter which is L_c.

AN ANALYTIC SOLUTION

Using a simple model for the velocity field, an analytic expression for charge density distributions can be obtained from equation (24). The solution is in integral form and may be applied to the case of a circular jet. Despite the sacrifices which are made to reach the analytic solution, the closed form solution already contains all the basic features of a circular, turbulent, charged jet.

Here, we intend to consider the combined effects of convection, turbulent diffusion and charge relaxation in an unrestricted jet disregarding the complexities that the flow field might introduce into the problem. To this end, we set

$$V_z(x, y) = V_j \tag{25}$$

and there will be no radial component for such a velocity field. Equation (24) is then reduced to

$$\frac{\partial q^*}{\partial z^*} - \frac{\kappa}{r^*}\frac{\partial}{\partial r^*}\left(r^*\frac{\partial q^*}{\partial r^*}\right) + \frac{1}{L_c}q^* = 0. \tag{26}$$

This equation is similar to the one considered by Danckwerts [17] who was studying simultaneous mass diffusion and chemical reaction. Subject to boundary conditions stated in equations (21), the solution for q^* is in integral form and contains Bessel functions J_0 of zeroth order;

$$q^*(r^*, z^*) = e^{-z^*/L_c} \times \int_0^\infty \int_0^1 \xi y\, e^{-\kappa z^* \xi^2} J_0(\xi y) J_0(\xi r^*)\, dy\, d\xi \tag{27}$$

with y and ξ being dummy variables of integration. The integration with respect to y can be carried out and equation (27) simplies to

$$q^*(r^*, z^*) = e^{-z^*/L_c} \int_0^\infty e^{-\kappa z^* \xi^2} J_0(\xi r^*) \cdot J_1(\xi)\, d\xi. \tag{28}$$

It is noted that the initial and boundary conditions are readily incorporated in the expression for q^* in equation (28) and the determination of q^* which involves a simple numerical integration can be undertaken irrespective of calculations for any other location in the flow. Simpson's rule is used to carry out the integration and generate charge density profiles for

this simplified case. One such series of profiles at various distances from the inlet of the jet is depicted in Fig. 1 when $L_c = 5$. For values of L_c larger than 500, the charge density profiles remain virtually similar to the profiles when $L_c = 500$. For this limit where $L_c \gg z^*$ in most of the flow region, the exponential term in front of the integral in equation (28) is almost unity; thus q^* becomes independent of L_c. Physically, this limit refers to the cases that the fluid conductivity is so low that no charge migration takes place and charged species are dispersed by convection and turbulent diffusion only. It then turns out that for $L_c > 500$, the last term in equation (26) which represents migration effects is much smaller than the other terms in the equation and can be dropped out. Charge density then obeys the conservation equation as mass and temperature and consequently charge density profiles should become self-preserved in the limit of large L_c. The individual curves for $L_c = 500$ are plotted in a normalized plane of q^*/q_{max} vs $r/r_{1/2}$ and presented in Fig. 2. Indeed, the overlap of the profiles at different z^* to one single curve in Fig. 2 demonstrates that the charge density distribution obeys a self-preservation law in the case when $L_c > 500$ and $L_c \gg z^*$. Fig. 1 describes another limit in which L_c is of order unity and the charged species due to strong effects of migration hardly extend to a distance of 10 jet radii from the jet inlet section.

Equation (28) can further be used to derive a simple expression for charge decay on the centerline axis. With $r^* = 0$, equation (28) reduces to

$$q^*_{max}(z^*) = e^{-z^*/L_c} \int_0^\infty e^{-\kappa z^* \xi^2} J_1(\xi)\, d\xi. \qquad (29)$$

The integral can be expressed in terms of the modified Bessel function $I_{1/2}$ and thus the final result becomes

$$q^*_{max}(z^*) = e^{-z^*/L_c}[1 - e^{-1/(4\kappa z^*)}]. \qquad (30)$$

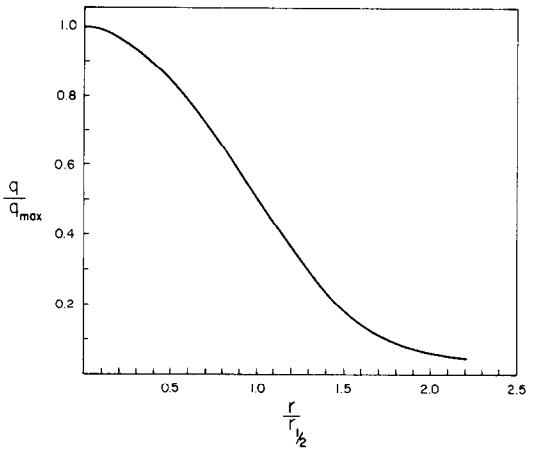

FIG. 2. Normalized charge density profiles using equation (28) with $L_c > 500$.

This equation is quite illuminating as it shows the combined effects of charge relaxation and turbulent diffusion in dispersion of charge in the flow. One is reminded that $\frac{1}{4}\kappa$ is approx. 10. With $L_c < 5$ which is the case when the fluid conductivity is relatively high ($\tau > \varepsilon V_j/5a$), the charge convected in the flow rapidly decays due to migration and diffusion plays an insignificant role. On the other hand, in the low conductivity limit of $\sigma > \varepsilon V_j/500a$, the charge species are dispersed by turbulent diffusion in the flow domain where $z^* \ll L_c$ which is in agreement with our previous conclusion.

Downstream of the inlet section, in the region $z^* > 20$, equation (30) can further be simplified. Expanding the exponential term in the bracket of equation (30) and keeping only the first two terms in the

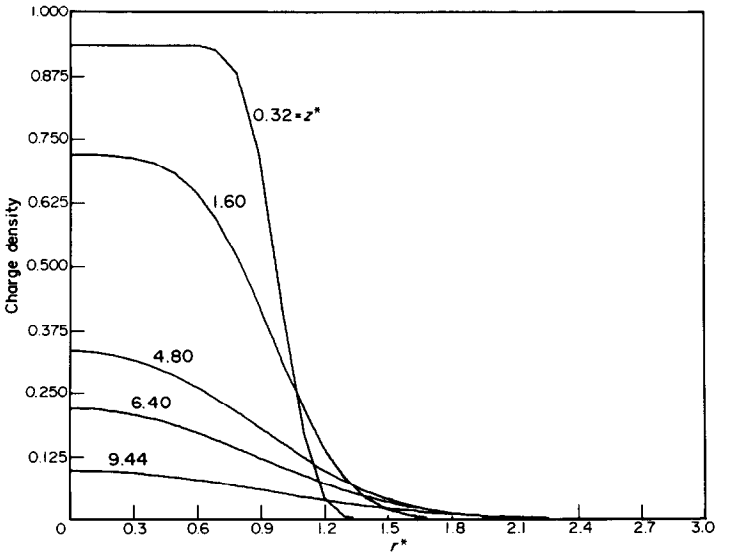

FIG. 1. Charge density profiles at jet cross sections with $L_c = 5.0$ using equation (28).

expansion, one finds that

$$q^*_{max}(z^*) = \frac{1}{4\kappa z^*} \cdot e^{-z^*/L_c} \tag{31}$$

at the centerline.

In this flow region, the charge density decays proportionally to the distance from the inlet section due to turbulent diffusion. Incidentally, in the limit $L_c \gg 1$ which the fluid is almost an electrically perfect insulator, and the dispersion of charged species is similar to other scalar quantities such as mass concentric and temperature, $q^*_{max}(z^*)$ obeys a decay law identical to the one described by equation (1) except for a constant which exists because of wall effects. Surprisingly, one also finds that the constant C_1 in equation (1) has the same numerical value as 4κ.

THE NUMERICAL SOLUTION

In this section, we confine our attempts to consider a realistic velocity profile and thereby numerically solve equation (22) for q^*. Obviously, a more comprehensive analysis involves an attempt to solve simultaneously equation (27) along with the Navier–Stokes equations and the continuity equations as is discussed, for example, by Spalding [10]. However, such an alternative does not appear practical in terms of computer time necessary to obtain a numerical solution in the entire flow field for different values of L_c. Besides, the present analysis is expected to be adequate for practical application which are concerned with the mean-charge density field and not the fluctuating part. The three different flow regions of a free turbulent jet issued from a submerged inlet is shown in Fig. 3. The inlet section extends $8a_j$–$10a_j$ from the inlet and is composed of a core potential region and a diffusion layer which grows with z. The axial velocity $z_{z,i}$ in the inlet section when $z^* < z_i^*$ can be expressed as follows [18]:

$$v^*_{z,i}(r^*, z^*) = \begin{cases} 1 & r^* < r_1^* \\ 2x^{1.5} - x^3 & r^* < r^* < r_2^* \\ 0 & r^* > r_2^* \end{cases} \tag{32}$$

where $x = (r_2^* - r^*)/(r_2^* - r_1^*)$ is the normalized thickness of the diffusion layer and the radii r_1^* and r_2^* which set the boundaries of the diffusion layer are defined as

$$\begin{aligned} r_1^*(z^*) &= 1 - \alpha z^* \\ r_2^*(z^*) &= 1 + \alpha z^* \end{aligned} \tag{33}$$

respectively with α being a constant. The parameter α is the rate of growth of the diffusion layer and it also determines the length of the inlet region. The radial distribution of the mean axial velocity becomes again self-similar beyond a distance $12a_j$–$16a_j$ from the inlet in a turbulent jet which is the established region and commonly known as the far field. The axial velocity v in the far field when $z^* > z_f^*$ is best approximated by [18]

$$v^*_{z,f}(r^*, z^*) = \frac{z_f^*}{z^*} \exp\left[-40(r^*/z^*)^2\right]. \tag{34}$$

The transitional region is situated between the inlet and far field sections of a turbulent jet where $z_i^* < z^* < z_f^*$. No specific expression for the velocity profile is available in this region; moreover, if one extrapolates $v_{z,i}$ and $v_{z,f}$ to the transitional region, it turns out that such a procedure will produce discontinuity in the axial velocity profiles. In the absence of any other alternatives, we define the axial velocity profiles in the transitional region by combining $v_{z,i}$ and $v_{z,f}$ through a weighting function. To be acceptable, the weighting function should be chosen in such a way that not only the velocity field becomes continuous in the entire flow domain, but also all its derivatives in the r and z directions be continuous. Thus, the following steps will

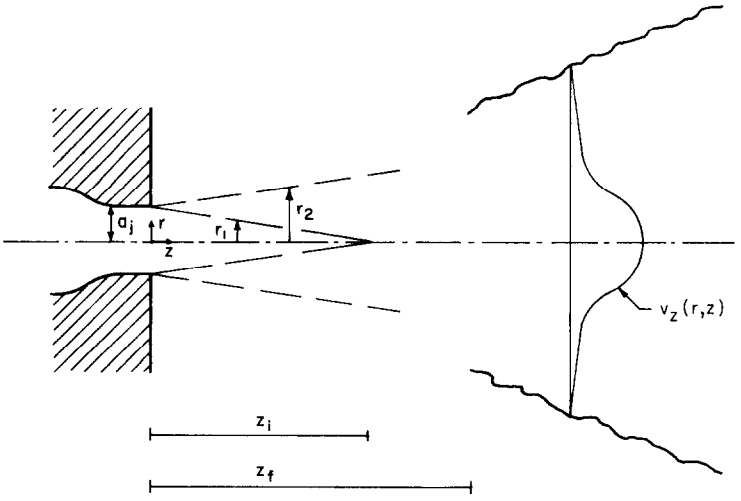

FIG. 3. Various regions in a turbulent jet.

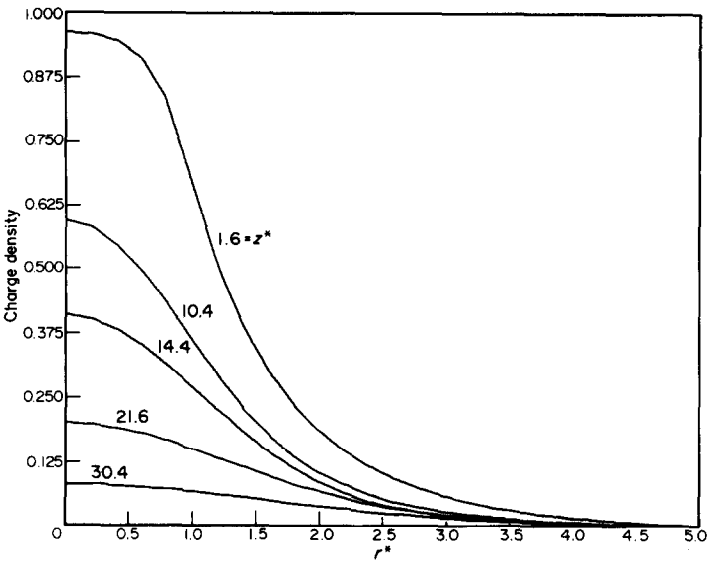

FIG. 4. Charge density profiles at several jet cross sections with $L_c = 50$, numerical solution.

be taken to define the velocity field in the transitional region. We set $z_f^* = 12.8$. Acccordingly, we also have

$$\alpha = \frac{1}{z_f^*} = 0.078. \tag{35}$$

For $z^* > 12.8$, $v_z(r^*, z^*)$ is determined from equation (3). When $z^* < 12.8$,

$$v_z^*(r^*, z^*) = v_{z,i}(r^*, z^*)[1 - e^{(z^* - z_f)/1.5}] + v_{z,f}^*(r^*, z_f^*)\, e^{(z^* - z_f^*)/1.5}. \tag{36}$$

This definition of v_z^* satisfies all the physical requirements for the velocity field. It matches the velocity profiles $v_{z,i}^*$ and $v_{z,f}^*$ at the proper limits and has a continuous derivative. It turns out, however, that the expression in equation (35) is in modest agreement with some of the experimental data as well [19].

The finite-difference procedure used to solve equation (24) is similar to the one developed by Patankar and Spalding [20], CDM in the radial direction and FMD in the axial direction, which leads

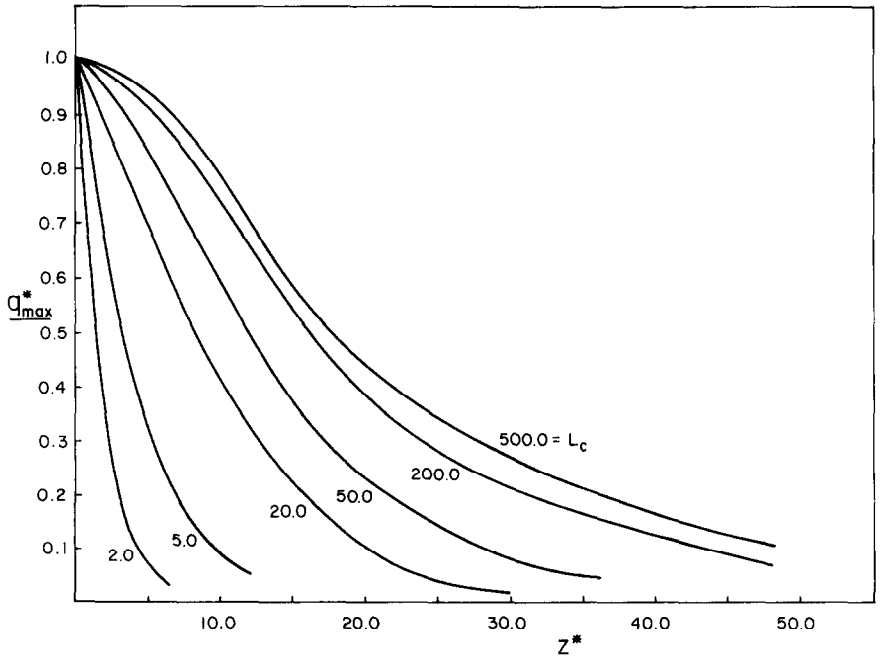

FIG. 5. The decay of q_{max} with z, numerical solution.

to an implicit scheme with no dependency on the downstream conditions. v_r^* is obtained using the continuity equation, equation (12). The numerical technique allowed for large steps in the axial direction with good stability in computations. For a more detailed description, one is referred to Davis [21].

Figure 4 presents the mean charge density profiles at several cross sections for $L_c = 50$. The radial charge density distributions in this figure demonstrate that all the initial and boundary conditions imposed on the problem are well satisfied. The computations also indicate that, in the far field, the charged fluid is confined to within five jet radii from the jet axis.

Variations of charge density on the centerline of the axisymmetric jet for different ranges of L_c are depicted in Fig. 5. Here, q^*_{max} is the ratio q_{max}/q_j with q_{max} being the maximum cross-sectional charge density which decreases monotonically as z^* increases. When $L_c < 5$, q^*_{max} decays rapidly in the inlet section. In this case, the fluid is sufficiently conductive and the charged species in the jet are dispersed via migration to the adjacent fluid and eventually to the walls of the container. For moderate ranges of L_c, i.e. $10 < L_c < 200$, the relaxation time τ is at least an order of magnitude larger than the characteristic time for convection a_j/V_j which allows for the simultaneous effects of migration and diffusion in the radial direction. The decay of q^*_{max} is dependent on L_c and is a result of relaxation as well as turbulent diffusion. In agreement with our analytical results presented previously, the characteristics of the charged jet remain independent of L_c for $L_c > 500$. In this limit, the relaxation time is much larger than the respective diffusion time scale and as a result migration effects are negligibly smaller in comparison to radial diffusion. With $L_c > 500$, the charge density field behaves similarly to conservative scalars, and the respective curve for decay of q^*_{max} may be compared with the experimentally observed decay of quantities such as temperature and concentration and qualitative agreements can be obtained for example with the experimental data of Birch *et al.* [11].

The spread of a charged jet can be presented by the variations of the jet half-radius of charge density profiles with z^*. These variations are shown in Fig. 6. This figure indicates that the charged jet actually shrinks when $L_c < 5$ and spreads to about twice its initial diameter when $10 < L_c < 200$. In the limit $L_c \geqslant 500$, the charged fluid tends to spread linearly in the far field up to $40a_j$ from the inlet: however, beyond this range, the time scale for convection is comparable to the relaxation time and as a result once again migration confines the charged jet.

CONCLUSIONS

Regarding the dispersion of charged species via a turbulent jet, three fluid conductivity ranges can be distinguished; a high conductivity limit when $\sigma > 0.2\ \varepsilon V_j/a_j$, an intermediate conductivity range when $0.005\ \varepsilon V_j/a_j < \sigma < 0.1\ \varepsilon V_j/a_j$, and finally a low conductivity range when $\sigma < 0.002\ \varepsilon V_j/a_j$ with σ and ε

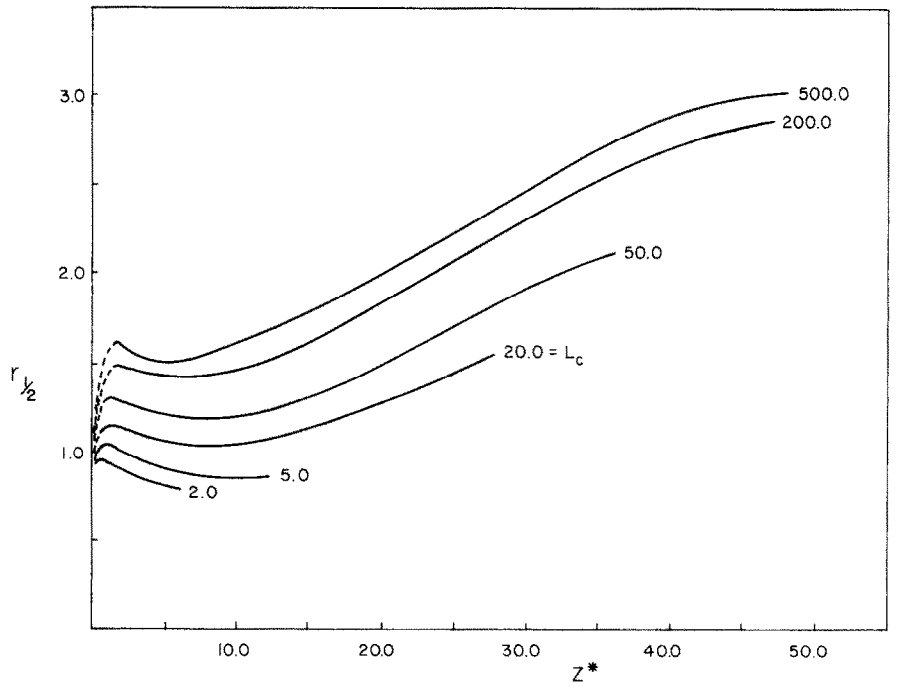

FIG. 6. The variation of $r_{1/2}$ with z, numerical solution.

being the fluid electrical conductivity and permittivity, respectively.

In the high conductivity limit, the induced electric field on the periphery of the jet disperses the charged species to the adjacent fluid and ultimately to the walls of the receiving vessel. The relaxation time is of the order of the characteristic time for convection a_j/v_j and as a result, the charge density decays rapidly in the near field of the jet and the charged fluid does not extend to the far field.

In the intermediate conductivity range, the charge relaxation time τ becomes comparable to the turbulent diffusion time scale which can be regarded as a_j^2/D_T. Further, in the immediate far field of the jet, the time scale z/V_j is of the same order as the other two time scales. Consequently, the charge density field is convected to the far field and in this region both migration and turbulent diffusion contribute to charge dispersion. Electrostatic characteristics of a charged jet, in this limit, are dependent on a dimensionless parameter L_c which is defined by equation (19); and the decay and spread of mean charge density in the jet is described in Figs. 5 and 6, respectively. The decay may also be obtained from equation (30) which is obtained using an approximate analytical solution.

For a turbulent charged jet, with $\sigma < 0.002\,\varepsilon V_j/a_j$, it can be considered that the fluid is almost an insulating one. Here, the relaxation time is much larger than the diffusion time; and as a result, migration effects are virtually non-existent except in the far downstream of the jet where the time scale z/V_j may be comparable to τ. Therefore, in this case, charge density profiles are independent of conductivity in the far field at least up to a distance of $100a_j$ downstream of the inlet section where charge density decays due to radial turbulent diffusion; and beyond this region, migration may again contribute to charge dispersion. One notes that, in this low-conductivity limit, sometimes high electric fields do exist on the jet boundaries; however, the fluid is also extremely resistive which makes the resulting radial migration current negligible in comparison to radial diffusion current.

For hazard applications, it is desirable to have an estimate of the charged region inside a receiving tank which is filled with charged fluid. As a useful byproduct of the present analysis, an assessment on the size of the charged fluid in a turbulent free jet can be made. Here, we are concerned with those regions in the flow that retain at least a specific fraction of the initial fluid charge density.

Noting that the charge density profile does not broaden itself appreciably downstream of the flow for all conductivity ranges, we may define an effective volume $\forall$ for the charged fluid in the jet as

$$\forall \equiv \pi a_j^2 L \tag{37}$$

with L being the axial distance from the inlet that $q_{max} = 0.1q_j$. In accordance with the definition in equation (37), Fig. 7 presents two curves for the variation of $\forall^*$ with respect to L_c which are the results of our numerical and analytical solutions. In this figure, $\forall^* = V/\pi a_j^3$ is the dimensionless volume. For both curves, $\forall^*$ increases with L_c up to the low-conductivity range of $L_c > 500$ where $\forall^*$ is independent of L_c and a constant. The value of $\forall^*$ in the low-conductivity range is 80 for the numerical solution and 160 for the

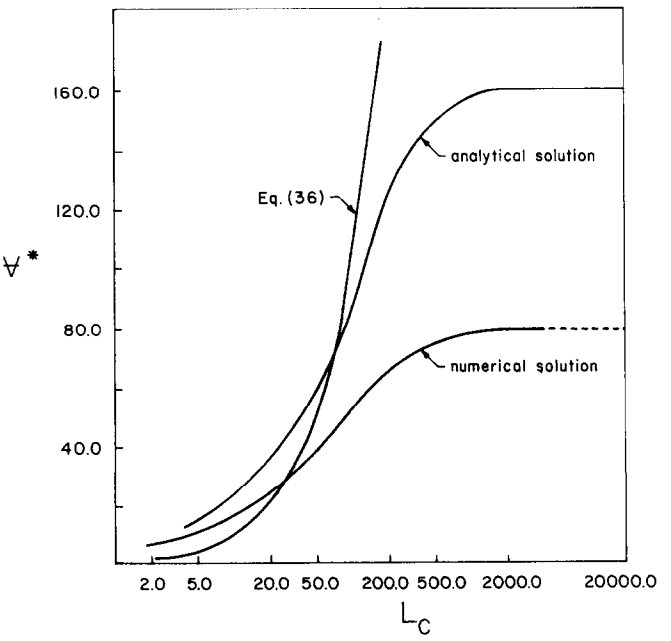

FIG. 7. The variation of $\forall^*$ in a turbulent jet.

analytic solution. It should be pointed out, however that the answer $\forall^* = 80$ for $L_c > 500$ is more acceptable and the overestimation of $\forall^*$ in the analytic solution stems from the simplified velocity field we considered for this analysis. Nonetheless, in the high conductivity limit, both of the curves obtained from the analytic and numerical solutions indicate that $\forall$ is proportional to τ. In their analysis of stationary charged clouds, Schon and Kramer concluded that the volume of charged fluid in a flow issued from a point source is roughly the product $\tau\dot{Q}$, with $\dot{Q}$ being the volume flow rate.

Regarding the jet problem, this assertion of Schon and Kramer will have the form

$$\forall = \pi a_j^2 v_j \tag{38}$$

and therefore,

$$\forall^* = L_c. \tag{39}$$

The variation of $\forall^*$ vs L_c as described by equation (39) is also included in Fig. 7. Our analysis predicts that equation (39) provides an approximation on the size of the charged fluid in the jet only in the high-conductivity range when migration and convection of charge are important. In other conductivity ranges that turbulent diffusion is a dominant factor in charge dispersion unrealistically high values for $\forall^*$ are obtained by using equation (39).

It might be desirable to address the effects of fluid charging level on the spreading and the decay, despite the fact that the small charge density limit covers the majority of instances in which electric charging effects occur in low conductivity fluids. While the fluid conductivity is constant in the small charge density limit, it varies with the local space charge as the charge density becomes comparable to the concentration of ionic species in the fluid. It can be shown [22] that the dependency between the conductivity and the charge density takes the special form,

$$\sigma = \sigma_0\left[\left(\frac{q}{FC_0}\right)^2 + 1\right]^{1/2} \tag{40}$$

when the ionic species are in thermodynamic equilibrium with the undissociated constituents. Equation (40) infers that the actual fluid conductivity increases with increasing charge density resulting in a net increase in the migration current. Furthermore, in the large charge density limit, the fluctuations of charge density in a turbulent flow induces corresponding fluctuations of conductivity which in turn produces *turbulent-eddy migration.*

Thus, with q being of order FC_0 or larger, the charge migration current is enhanced by an actual increase in the fluid conductivity and also by the presence of turbulent-eddy migration. The influence of this enhancement on our results is that it shifts the transition from high to low conductivity limits to higher L_c values than the ones predicted from the small charge density limit. The extent of this shift depends on the initial charging level in the jet.

One is reminded that with the mixing and decay, the fluid retains small portions of the initial charge in much of the downstream section and at the jet boundaries. Then, the small charge density limit analysis still can be applied in these regions. Nonetheless, to incorporate the effects of large charge densities in our results, we suggest that *as a first guess* L_c may be alternatively considered as

$$\varepsilon V_j \Big/ \left\{a_j\sigma_0\left[\left(\frac{q_j}{FC_0}\right)^2 + 1\right]^{1/2}\right\}.$$

Finally, we should add that the application of the present work may be limited by the simplifying assumption used to develop the theory; and therefore, the results presented here can be used more effectively when these assumptions are also considered in applications. With regard to charged species we have assumed that: (1) positive and negative ionic species have equal molecular diffusion coefficients; (2) the local imbalance of positive and negative charged species which generate a charge field is always much less than the concentration of ionic species themselves, i.e. small charge density limit applies, yet the theory may be used as a first guess for jets with initially large charging levels by redefining L_c as suggested above; (3) the charging interaction between the fluid and the walls of the receiving tank can be neglected. With respect to the flow field, the assumptions are: (4) the turbulent eddy-viscosity and the turbulent eddy diffusion coefficient are equal; (5) the velocity profile in the transition region of a turbulent jet can be approximated by bridging the velocity profiles in the inlet and the established regions; and (6) the charge density at the inlet of the turbulent jet is uniform.

REFERENCES

1. R. S. Roy, A perspective on electrochemical phenomena. In *Advances in Heat Transfer*, Vol. 12, pp. 196–277. Academic Press, New York (1976).
2. J. T. Leonard, Generation of electrostatic charge in fuel handling systems: a literature survey, Naval Research Laboratory Report 8484 (September 24, 1981).
3. J. P. Wagner, Charge generation and transport during flow of low conductivity fluids. In *Handbook of Fluids in Motion*, N. P. Cheremisinoff and R. Cupta (Editors), Chap. 41, Ann Arbor Science, Ann Arbor, Michigan (1983).
4. B. Abedian, Electrostatic charge relaxation in tank filling operations, *J. Electrostat.* **14,** 35–57 (1983).
5. S. Corrsin and M. S. Uberoi, Further experiments, on the flow and heat transfer in a heated turbulent air jet, N.A.C.A. Tech. Note No. 1865 (1949).
6. D. Kristmanson and P. V. Danckwerts, Studies in turbulent mixing—I. Dilution of a jet, *Chem. Engng Sci.* **16,** 267–277 (1961).
7. R. A. Wilson and P. V. Danckwerts, Studies in turbulent mixing II. A hot air jet, *Chem Engng Sci.* **19,** 885–895 (1964).
8. J. O. Hinze and B. G. Hegge Zijnen, Transfer of heat and matter in the turbulent mixing zone of an axially symmetrical jet, *Appl. Sci. Res.* **A1,** 435–460 (1949).

9. A. H. Becker, C. H. Hottel and C. G. Williams, The nozzle fluid concentration field of the round turbulent free jet, *J. Fluid Mech.* **30,** 285–303 (1967).
10. D. B. Spalding, Concentration fluctuations in round turbulent free jet, *Chem. Engng Sci.* **26,** 95–107 (1971).
11. A. D. Birch, D. R. Brown, M. G. Dodson and J. R. Thomas, The turbulent concentration field of a methane jet, *J. Fluid Mech.* **88,** 431–449 (1978).
12. R. J. Santoro, H. G. Semerjian, P. J. Emmerman and R. Goulard, Optical tomography for flow field diagnostics, *Int. J. Heat Mass Transfer* **24,** 1139–1150 (1981).
13. G. Schon and H. Kramer, On the size of stationary space charge clouds in streaming media. *Proc. 3rd Conference on Static Electrification.* Inst. Phys. Conf. Ser. No. 14 (1971).
14. P. A. Libby and F. A. Williams, Fundamental aspects. In *Turbulent Reacting Flows*, Chap. 1. Springer-Verlag, Berlin (1980).
15. A. G. Bailey and W. Balachandran, The disruption of electrically charged jets of viscous liquid, *J. Electrostat.* **10,** 99–105 (1981).
16. I. Wygnanski and H. Fiedler, Some measurements in the self-preserving jet, *J. Fluid Mech.* **38,** 577–612 (1968).
17. P. V. Danckwerts, Adsorption by simultaneous diffusion and chemical reaction into particles of various shapes and into falling drops, *Trans. Faraday Soc.* **47,** 1014–1923 (1951).
18. G. N. Abramovich, *The Theory of Turbulent Jets*, Chap. 5. MIT Press, Cambridge, Mass. (1963).
19. S. Sami, Balance of turbulence energy in the region of jet-flow establishment, *J. Fluid Mech.* **29,** 81–92 (1967).
20. S. V. Patankar and D. B. Spalding, *Heat and Mass Transfer in Boundary Layers.* Morgan-Grampian, London (1967).
21. E. S. Davis, Analysis of a charged turbulent free jet. M.S. thesis, Tufts University (1983).
22. J. Gavis, Relaxation of electrically charged hydrocarbon liquids, *Chem. Eng. Sci.* **22,** 633–635 (1967).

CARACTERISTIQUES ELECTROSTATIQUES D'UN JET LIBRE, TURBULENT CHARGE

Résumé—On étudie l'expansion et la dégénérescence d'un fluide chargé qui pénètre dans un fluide en repos. L'équation de conservation dynamique des charges est résolue analytiquement pour le champ de densité de charge moyenne dans l'écoulement en supposant un champ de vitesse simple et aussi numériquement en utilisant un champ de vitesse plus précis. On montre que les caractéristiques d'un jet chargé peuvent être décrites par un rapport adimensionnel de longueur $(\varepsilon V_j)/(\tau a_j)$, ε et τ étant la permittivité et la conductivité électriques du fluide. On identifie trois domaines de conductivité à partir des propriétés électrostatiques d'un jet chargé. Dans le domaine de conductivité élevée, quand $\tau > 0{,}2(\varepsilon V_j/a_j)$, la région chargée est confinée seulement au champ proche. A l'autre extrême, pour $\tau < 0{,}002(\varepsilon V_j/a_j)$, il y a un domaine de basse conductivité dans lequel le champ de densité de charge dans l'écoulement a un comportement analogue à d'autres champs scalaires conservatifs dans un jet turbulent avec des vitesses de décroissance et d'élargissement semblables. Le domaine intermédiaire de conductivité est placé entre ces deux limites et la dispersion de charge est contrôlée par la migration et la diffusion.

ELEKTROSTATISCHE EIGENSCHAFTEN EINES ELEKTRISCH GELADENEN TURBULENTEN FREISTRAHLS

Zusammenfassung—Die Aufweitung und der Zerfall eines geladenen Fluids, das als frei eintauchender, turbulenter Strahl in ein ruhendes Fluid einströmt, werden untersucht. Die dynamische Erhaltungsgleichung der Ladung wird für das Feld der mittleren Ladungsdichte in der Strömung sowohl analytisch—bei Annahme eines einfachen Geschwindigkeitsfeldes—als auch numerisch—für ein genaueres Geschwindigkeitsfeld—gelöst. Es wird gezeigt, daß die Eigenschaften eines geladenen Strahls durch ein dimensionsloses Längenverhältnis beschrieben werden können, das definiert ist als $(\varepsilon V_j)/(\sigma a_j)$, wobei ε die elektrische Dielektrizitätskonstante und σ die elektrische Leitfähigkeit des Fluids ist. Aufgrund der elektrostatischen Eigenschaften des geladenen Strahls konnten drei Leitfähigkeitsbereiche unterschieden werden. Ein Bereich hoher Leitfähigkeit, für $\sigma > 0{,}2\ \varepsilon V_j/a_j$, in dem die geladene Zone auf das nähere Umfeld beschränkt ist. Das andere Extrem, für $\sigma < 0{,}002\ \varepsilon V_j/a_j$, ein Bereich niedriger Leitfähigkeit, in dem sich das Feld der Ladungsdichte in der Strömung analog zu anderen eingeprägten Skalarfeldeigenschaften in einem turbulenten Strahl mit ähnlichen Aufweitungs- und Zerfallsraten verhält. Der Bereich mittlerer Leitfähigkeit liegt zwischen diesen beiden Grenzen, dort wird die Ladungsverteilung durch die Bewegung und Diffusion bestimmt.

ЭЛЕКТРОСТАТИЧЕСКИЕ ХАРАКТЕРИСТИКИ ТУРБУЛЕНТНОЙ СВОБОДНОЙ СТРУИ ЗАРЯЖЕННОЙ ЖИДКОСТИ

Аннотация—Исследуется распространение и затухание заряженной турбулентной затопленной струи. Динамическое уравнение сохранения заряда решается аналитически для поля средней плотности заряда в потоке в предположении простого поля скоростей, а также численно при использовании более реалистичного поля скорости. Показано, что характеристики струи заряженной жидкости могут быть описаны с помощью безразмерного параметра $(\varepsilon V_j)/(\sigma V_j)$, где ε и σ диэлектрическая проницаемость и электропроводность жидкости, соответственно. На основе электростатических свойств струи заряженной жидкости найдены три характерных области заряженной струи. В диапазоне высокой проводимости, где $\sigma > 0{,}2(\varepsilon V_j)/a_j$, заряженная область сосредоточена только в ближнем поле. В другом диапазоне, где $\sigma < 0{,}002\ (\varepsilon V_j)/a_j$, существует область низкой проводимости, поле плотности заряда которой ведет себя аналогично другим скалярным полям в турбулентной струе с теми же скоростями вырождения и расширения струи. Область промежуточной проводимости находится между двумя указанными зонами, причем дисперсия заряда в ней определяется балансом между миграцией заряда и турбулентной диффузией.